ABSORBER FOAM CHARACTERIZATION FOR PREDICTING OVERALL ANECHOIC CHAMBER PERFORMANCE

Christopher R. Brito
Lockheed Martin
1111 Lockheed Martin Way, Sunnyvale, CA 94089

Aloysius Aragon Lubiano
Raytheon, 2000 East Imperial Highway
RE/R01/A566, El Segundo, CA 90245

Newlyn Hui
L3 Communications, Randtron Antenna Systems
130 Constitution Dr., Menlo Park, CA 94025

Dean Arakaki
California Polytechnic State University
1 Grand Avenue, San Luis Obispo, CA 93407

ABSTRACT

A new rectangular anechoic chamber (20'L x 10'W x 9'7"H) has been established at California Polytechnic State University (Cal Poly) through donations and financial support from industry and Cal Poly departments and programs. The chamber was designed and constructed by three graduate students as part of their thesis studies to explore and further their understanding of chamber design and antenna measurements. The chamber project has included RF absorber characterization, overall chamber performance assessment, and software development for the coordination of a positioner with a vector network analyzer.

This paper presents absorber characterization as a function of incidence angle and orientation to enable an overall chamber performance analysis. Test data at low incidence angles (< 30^{o}) are compared to manufacturer performance curves at normal incidence. The mean response of the measured data indicates a correlation with manufacturer curves. Through ray tracing analysis, the ripple encountered in the test data is used to identify two effective reflection planes indicative of the foam geometry. The measured data are subsequently used to predict overall anechoic chamber performance to within 1dB for a majority of the actual scan data. Details of this analysis and comparisons to actual chamber performance are presented in a companion paper.

Keywords: Absorber material, Absorber shape effects, Anechoic Chamber, Reflectivity, IEEE 1128 Standard.

1.0 Introduction

During radiation pattern testing inside an anechoic chamber, radiation emanating from the source antenna reaches the antenna under test (AUT) directly and via multiple reflection paths. To predict overall anechoic chamber performance, absorber reflectivity is required at the oblique incidence angles and at orientations encountered by radiation incident on the chamber walls along these reflection paths [1]. Due to the availability of foam shapes (insufficient number of pyramid-shaped foam), wedge-shaped foam was installed on the chamber walls outside the specular (one-bounce reflection) regions. Therefore, both the wedge- and pyramidal- shaped absorber foam is characterized with respect to orientation, incidence angle, and frequency.

2.0 Approach

Absorber reflectivity is measured using the industry standard test fixture illustrated in Fig. 1 below.

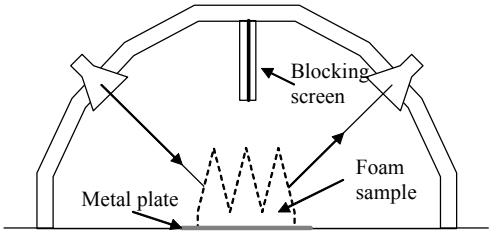

Fig. 1: Absorber Test Fixture

This structure, known as the NRL arch [2], has a 5' radius and allows an incidence angle resolution of 10° at horizontal and vertical polarizations for the source and receive horn antennas. For the frequency ranges 2.6GHz to 3.95GHz and 3.95GHz to 5.85GHz, pairs of Narda 644 and 643 standard gain horns are used, respectively. The fixture is calibrated with respect to a 4' x 4' metal plate centered under the arch to provide a baseline reference prior to foam reflectivity measurements, as per the IEEE 1128 standard [3].

To reduce errors in the foam reflected signal, the direct path between the horn antennas is eliminated by placing a metal backed two-sided flat absorber between the two antennas. To minimize other extraneous reflections, the entire structure is placed within the anechoic chamber.

Both wedge- and pyramid-shaped absorber foam are measured with respect to the baseline metal plate. The horn pairs are fixed at vertical polarization while absorber foam orientation is varied from co- to cross-pol: aligned and normal to incident polarization, respectively.

3. Test Results

To verify measurement accuracy, pyramid absorber foam is first measured at normal incidence as a function of electrical thickness and compared to manufacturer standards. A comparison to manufacturer standards, taken at discrete frequency values, is shown in Fig. 2 below.

The curves in Fig. 2 illustrate a close correlation between measured and manufacturer specifications up to a reflectivity level of 50dB. Measurements at this level are limited by the dynamic range of the network analyzer. The plot marked by triangles is a standard curve from [1] developed by the author from absorber manufacturer data. The manufacturer data was obtained from AEMI [4]. These curves are used as a reference for expected performance.

Measurements were taken at 20° and 30° oblique incidence angles for 24" height pyramid and wedge shaped foam over the frequency range 2.6GHz to 3.95GHz (401 points).

Measured data is presented for 24" height pyramid foam in both normal and twisted configurations. Wedge foam data is presented for orientations in which the incident electric field is co-pol and cross-pol to the direction of the wedges. The data presented in the following figures also contains the manufacturer and standard curves from Fig. 2 for reference.

Reflectivity data collected for 24" pyramid data shows that the twisted configuration (Fig. 4) pyramid foam performs 1.5-4.5dB better than a square orientation (Fig. 3). It has been suggested in [1] that this improvement is due to the reduction of forward scatter. This foam analysis led to the decision of using twisted pyramid foam in the specular regions of the Cal Poly Anechoic Chamber.

Reflectivity data was collected for wedge foam in both the co-pol and cross-pol orientations. Although the reflectivity in the cross-pol orientation (Fig. 5) was found to be comparable to that of the pyramid foam, co-pol reflectivity (Fig. 6) was 7-9dB lower than the pyramid foam results. These findings justify wedge foam usage only in areas outside the specular region.

The measurements include ripple (Fig. 7) caused by the interference between two effective reflection planes created by the foam structure. The two reflection paths contributing to the interference pattern are shown in Fig. 4.

4. Ripple Analysis

The diagram in Fig. 8 indicates a potential secondary reflection plane created by the tips of the pyramid foam structure. This secondary source of reflections interferes with those emanating from the primary reflection plane located at the base of the pyramids. These signals combine to create the ripple pattern found in Fig. 7.

A diagram showing the location of the two assumed reflection planes relative to the source and receive horn antennas is shown in Fig. 9. Given the height of the primary reflection plane (base of pyramids), the height of the secondary reflection plane is determined by computing the difference in the propagation distances between the primary and secondary reflected signals.

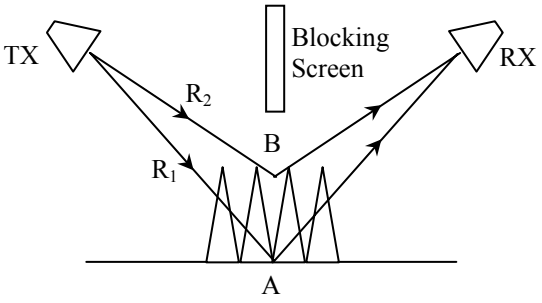

Fig. 8: Multiple Reflection Paths

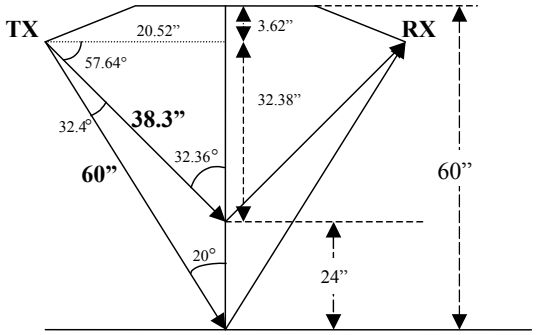

Fig. 9: Multiple Reflection Path Geometry

Since both signals are reflected by the absorber foam, the phase of the reflection coefficients is approximately the same for both reflections. For in-phase signals, cancellation (destructive interference) occurs when the difference in path length ΔR is an odd multiple of a half-wavelength.

$$\Delta R = R_2 - R_1 = (2n+1)\frac{\lambda}{2} \qquad (1)$$

Where n is an integer. Therefore, the frequencies where signal cancellation occurs is given by:

$$f = \frac{c}{2}\frac{2n+1}{\Delta R} \qquad (2)$$

Using both the dimensions defined in Fig. 9 and equation (2), the frequencies at which reflectivity peaks (minimum reflection levels) are predicted to occur include 2.86, 3.14, 3.41, and 3.68GHz. The measured reflectivity peaks occur (Fig. 7) at approximately 2.88, 3.15, 3.43, and 3.67GHz. The close correlation confirms the existence of a secondary reflection plane at the tips of the pyramid structure.

5. Conclusions

This paper has presented an extension to manufacturer data generally available on the performance of absorber foam used in anechoic chambers. Test measurements at normal incidence are compared to manufacturer specifications to verify measurement accuracy. Characterization data is then taken over an extended range of test conditions including multiple oblique incidence angles, foam orientations, and frequency ranges.

Significant ripple is noticed in the test measurements and is used to predict the existence of a secondary reflection plane. This plane is predicted and confirmed to be at the tips of the pyramid structure. The acquired reflectivity data will be used in a subsequent analysis of the overall reflectivity performance of the entire anechoic chamber.

6. REFERENCES

[1] Hemming, L.H., *Electromagnetic Anechoic Chambers*, Piscataway, NJ: IEEE Press, 2002.

[2] Emerson, W.H., "Electromagnetic Wave Absorbers and Anechoic Chambers Through the Years," *IEEE Trans. Antennas Propagat.*, vol. AP-21, no. 4, p. 484, July 1973.

[3] *IEEE Std 1128-1998*, IEEE Recommended Practice for Radio-Frequency (RF) Absorber Evaluation in the Range of 30 MHz to 5 GHz. 1998, New York: IEEE Press.

[4] Advanced Electromagnetics, Inc, *www.aemi-inc.com, 2003*

7. ACKNOWLEDGMENTS

The authors would like to thank Deskin Research, Raytheon, and Lockheed Martin for material donations and the employees of Lockheed Martin and JPL for technical support during the construction and testing of the Cal Poly Anechoic Chamber. We would also like to thank Cal Poly's Center for Teaching and Learning for support through the University Summer Services and Fall Faculty Development Grant Programs and Cal Poly's Electrical Engineering Department for financial support of the chamber project through the purchase of absorber foam.

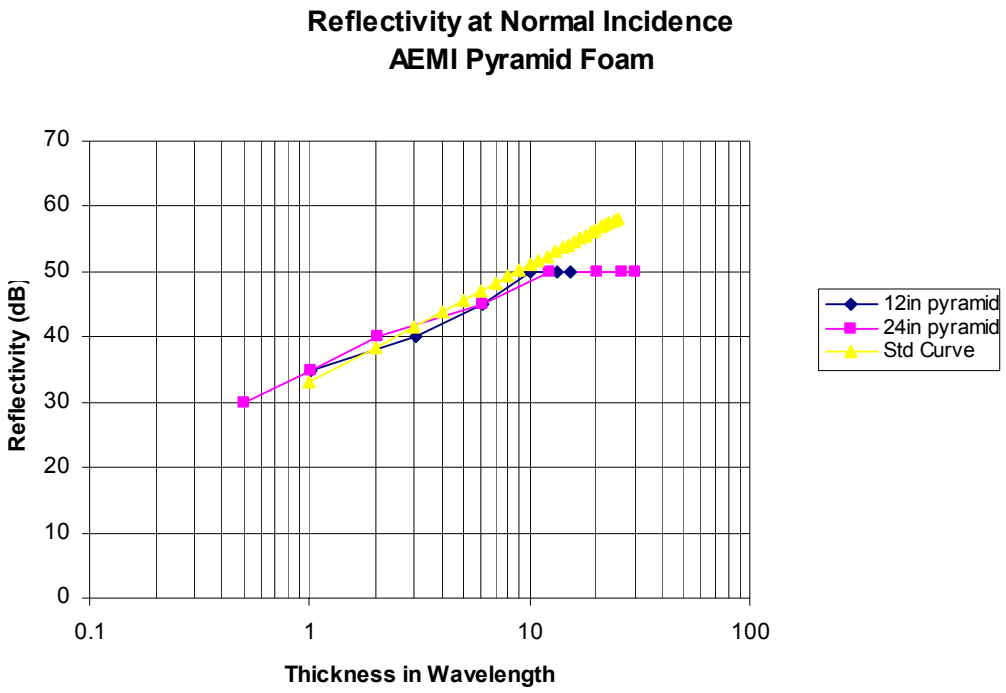

Fig. 2: Reflectivity of AEMI Pyramid Foam

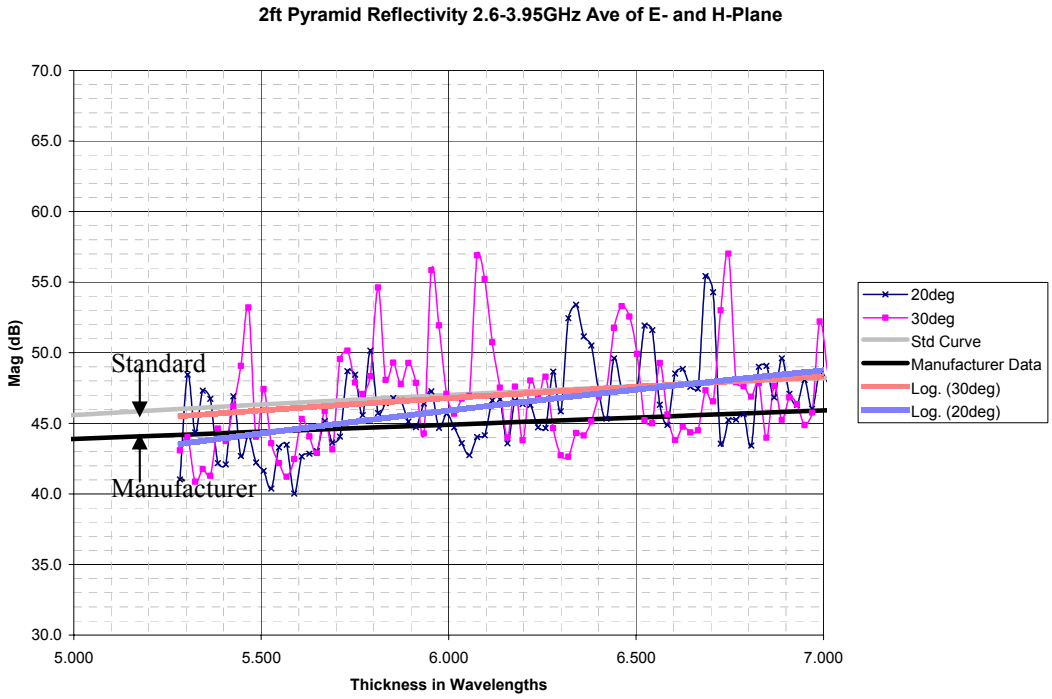

Fig. 3: 24" Pyramid Reflectivity Data

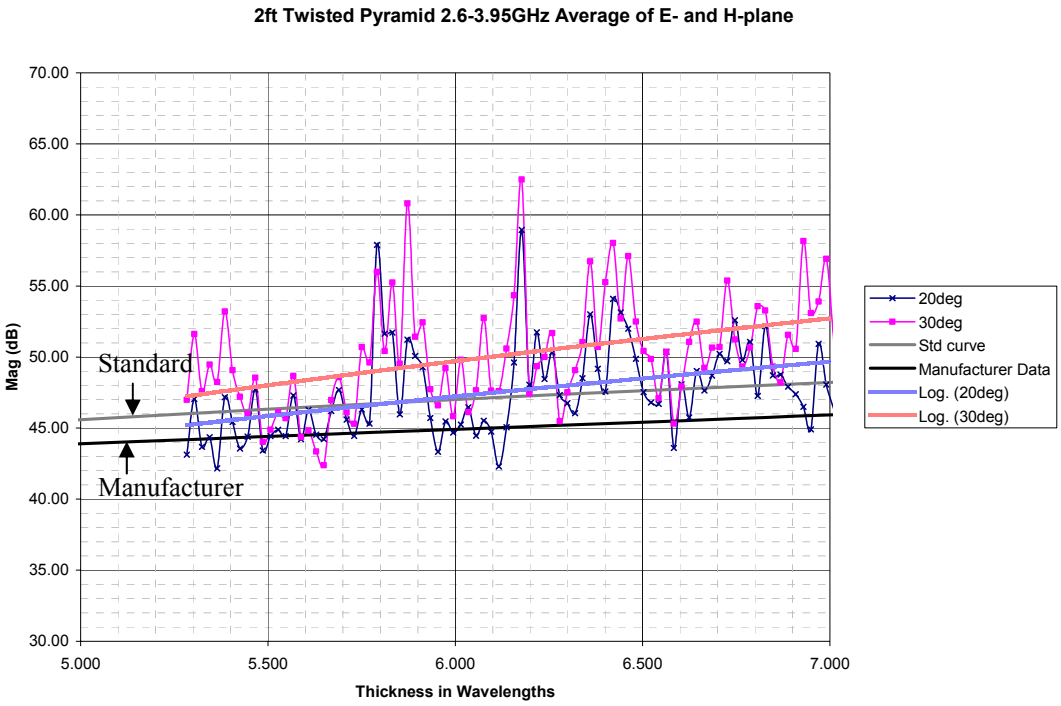

Fig. 4: 24" Pyramid Reflectivity Data (Twisted Configuration)

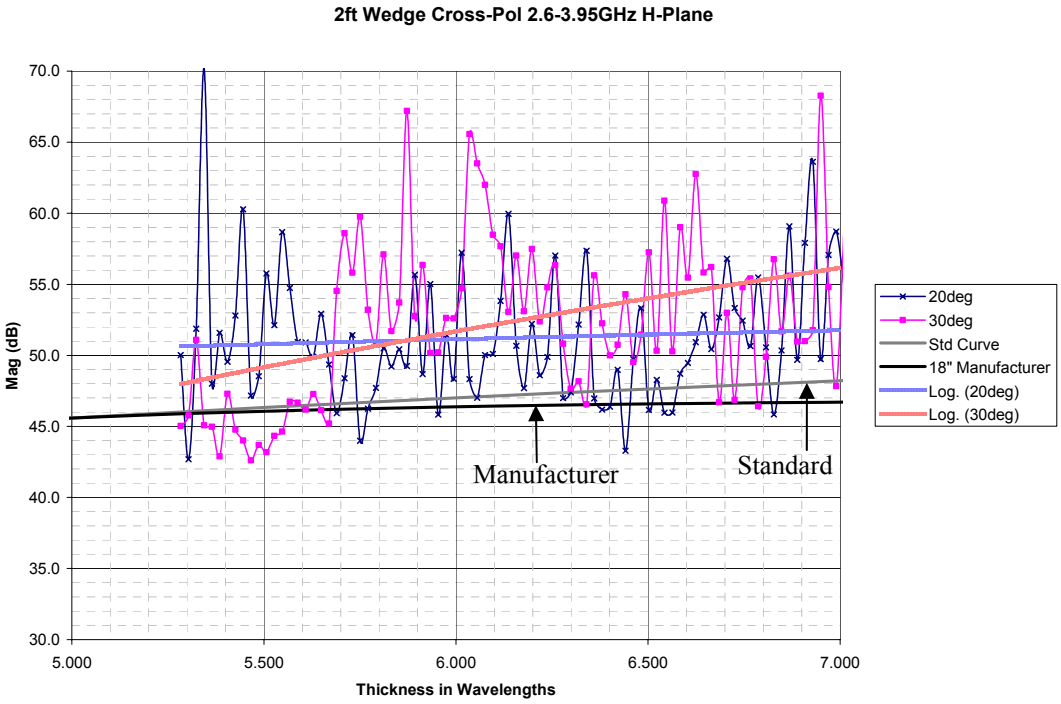

Fig. 5: 24" Wedge Reflectivity Data (Cross-pol)

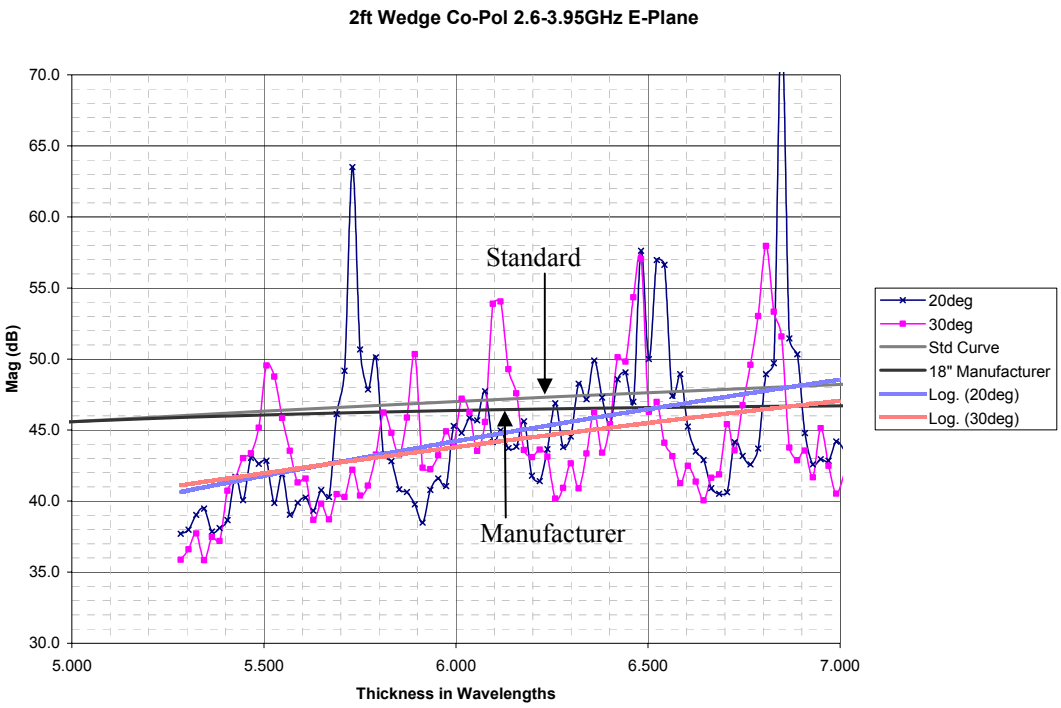

Fig. 6: 24" Wedge Reflectivity Data (Co-pol)

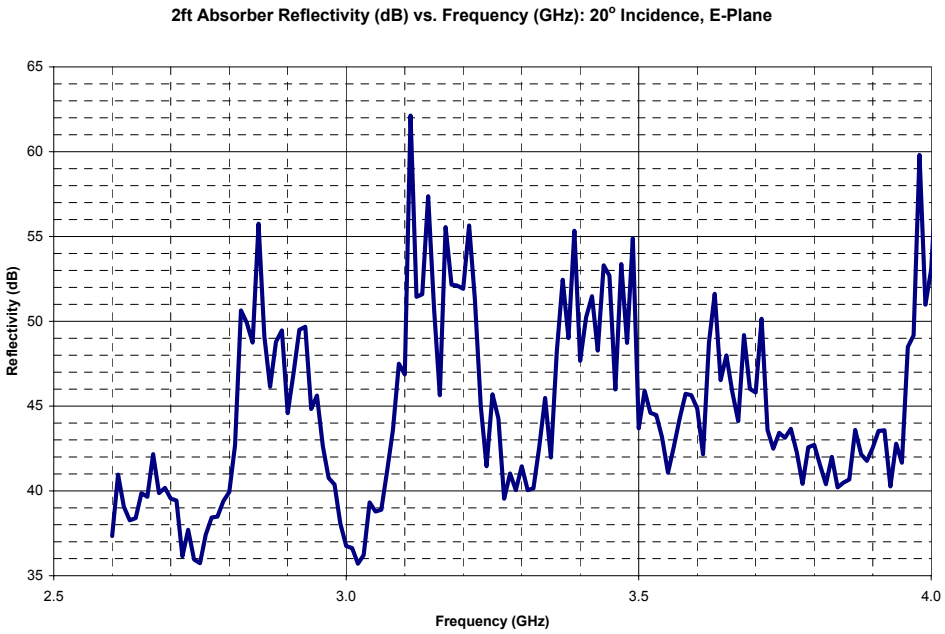

Fig. 7: 2ft-Height Pyramidal Absorber Reflectivity